Practical Electronic Noses Through Integration of Selective Semipermeable Membranes with Organic Field Effect Transistors

Mallory Mativenga[*] and Bright Walker[**]
[*]Department of Information Display, Kyung Hee University, Seoul 02447, Republic of Korea
E-mail: mallorykr@gmail.com
[**]Department of Chemistry, Kyung Hee University, Seoul, 02447, Republic of Korea
E-mail: walker@khu.ac.kr

Abstract
Electronic noses (E-noses) mimic olfactory organs and detect volatile organic compounds (VOCs) for applications in environmental monitoring, healthcare, and food safety. Organic field-effect transistor (OFET) sensors offer an economical platform for large-scale production, but their selectivity remains a challenge. In this study, we incorporate semi-permeable polymer membranes into OFET vapor sensors to enhance analyte differentiation. Acylated poly(vinyl alcohol) (PVA) derivatives were synthesized, characterized, and applied as selective membranes. By monitoring drain current over time, we demonstrated that these membranes significantly improved sensor selectivity, particularly in distinguishing similar VOCs such as methanol and ethanol. This strategy enables cost-effective fabrication of highly selective organic vapor sensors by modulating membrane properties.

Author Keywords
Conjugated polymer; field effect transistor; organic semiconductor; vapor sensor; electronic nose.

1. Introduction
Electronic sensors, including touch sensors, optical cameras, strain gauges, motion sensors, and speech detectors, are at the core of most automated or interactive systems.[1] In display devices, for example, most of these sensors are not only integrated on the devices for better user experience but are also required during their manufacture and processing.[2–4] Although most sensors in the realms of touch, speech, motion, strain, and vision are now mature technologies with exceptional precision, chemical sensors that emulate the senses of smell or taste are relatively underdeveloped. The need for chemical sensors in modern technologies continues to increase, while mimicking the human sense of smell has yet to be realized. Electronic noses, which combine sensor arrays with machine learning, have the potential to identify VOCs in a wide range of environments including in the food industry(sensing ripeness, spoilage, quality, allergens), defense (sensing chemical weapons, explosives) and healthcare (sensing disease bioindicators).[5] Despite progress, E-nose commercialization has been hindered by fabrication costs and limited selectivity. Current sensor platforms, such as metal oxide semiconductor (MOS) sensors, require high operating temperatures and suffer from broad, non-specific responses to different analytes.[4] OFET-based sensors offer a promising alternative, with advantages including flexibility, solution processability, and low power consumption.[6,7]

A primary drawback of OFET sensors is their low selectivity due to non-specific interactions between VOCs and the organic semiconductor layer. In this work, we demonstrate the use of semi-permeable polymer membranes to enhance selectivity by modulating analyte diffusion. Inspired by biological olfaction, where odorants interact selectively with receptors,[8] we hypothesize that polymer membranes with tailored functional groups can facilitate selective transport of analytes to the active sensing layer. This strategy enables the design of diverse, highly selective vapor sensors without requiring extensive synthesis of new conjugated polymers. The concept is illustrated in Figure 1, which shows how membranes which selectively transmit different types of analytes can be used to discriminate different types of analytes using a single type of detecting layer. A more detailed investigation of this topic has been published separately.[9] Note that the conceptual diagram implies that the membranes exclude molecules based on shape, however, the membranes in this study exclude molecules via chemical interactions.

2. Materials and Methods
Synthesis of Acylated PVAs: Poly(vinyl alcohol) (PVA) was functionalized via esterification with various acyl chlorides to

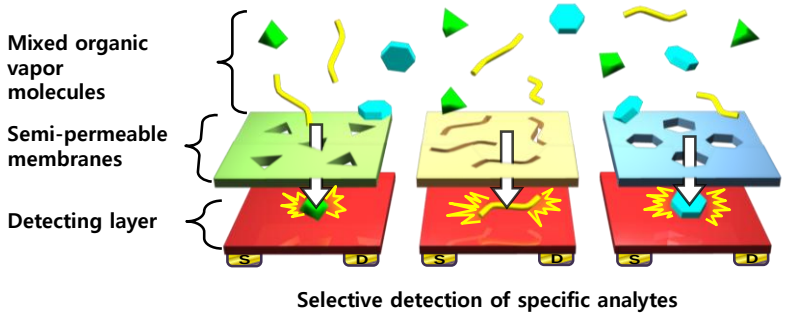

Figure 1. Schematic diagram showing the use of semi-permeable membranes to allow selective transmission of analytes to a detecting layer. Reproduced with permission from [9].

ISSN 0097-996X/25/5601-0373-$1.00 © 2025

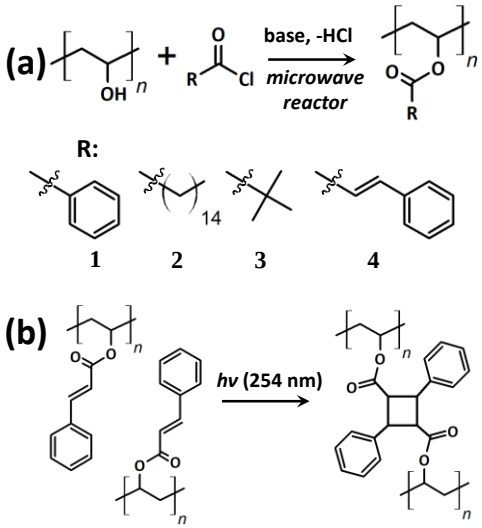

Figure 2. Synthesis of PVA derivatives used as membranes in this work. Reproduced with permission from [9].

obtain derivatives with different functional groups, including poly(vinyl benzoate) (PVBenzoate), poly(vinyl palmitate) (PVPalmitate), poly(vinyl pivalate) (PVPivalate), and poly(vinyl cinnamate) (PVCinnamate). Reactions were accelerated using microwave heating, allowing complete acylation within minutes. Cross-linked PVCinnamate films were obtained by UV irradiation. The synthetic conditions for these polymers are summarized in Figure 2.

Device Fabrication: OFETs were fabricated on glass substrates with inverted coplanar architecture. PBTTT was used as the semiconducting layer, while acylated PVAs were deposited as membranes. Electrical characterization was performed before and after vapor sensing tests.

Vapor Sensing Experiments: Seven different VOCs with a range of polarities and chemical structures were used in this study including methanol, ethanol, hexane, toluene, tetrahydrofuran (THF), methyl ethyl ketone (MEK), and ethyl acetate (EA). A controlled vapor delivery system ensured reproducible analyte exposure at known partial pressure. I_{DS} (drain current) was measured over time to evaluate sensor responses. A diagram showing the system for testing FETs upon exposure to different analytes is shown in Figure 3. Raw I_{DS} data produced by a sensor with no membrane is shown in Figure 4a. Because of drift in the I_{DS} data over long periods of time, data was normalized. One of the biggest impacts of the membranes was to modulate the time period over which the I_{DS} data changed, therefore, normalized data was fit with exponential decay curves to quantify membrane effects on time response. Figure 4b shows a representative comparison of devices without and with PVBenzoate membranes exposed to THF vapor, yielding time constants of 4.4 and 22.7 seconds, respectively. All of the membranes caused consistent shifts in such time constants; these shifts were influenced by the chemical structure of the membrane much more strongly than the film thickness.

3. Results and Discussion

Selectivity Enhancement by Membranes: CP FET sensors without membranes exhibited nearly identical responses to different VOCs, clearly illustrating the poor selectivity of OFET vapor sensors without membranes. Upon introducing acylated PVA membranes, unique sensor responses emerged for each analyte.

Differentiation of Methanol and Ethanol: Differentiating methanol and ethanol is notoriously difficult due to their structural similarity. However, CP FET sensors with cross-linked PVCinnamate membranes showed significant differences in response kinetics. The initial response slopes were 0.0403 s^{-1} for methanol and 0.0192 s^{-1} for ethanol (6σ confidence), while decay constants differed by over 26σ. These results indicate that membrane-functionalized sensors can reliably distinguish between structurally similar VOCs.

Membrane Effects on Hydrophobic VOCs: Hexane, a nonpolar molecule, was effectively blocked by PVBenzoate, PVPivalate, and PVCinnamate membranes. In contrast, PVPalmitate allowed hexane diffusion, which can be attributed to the similar aliphatic structure of both PVPalmitate and hexane. This demonstrates that membranes can be designed to selectively permit or inhibit analyte diffusion based on chemical similarity or

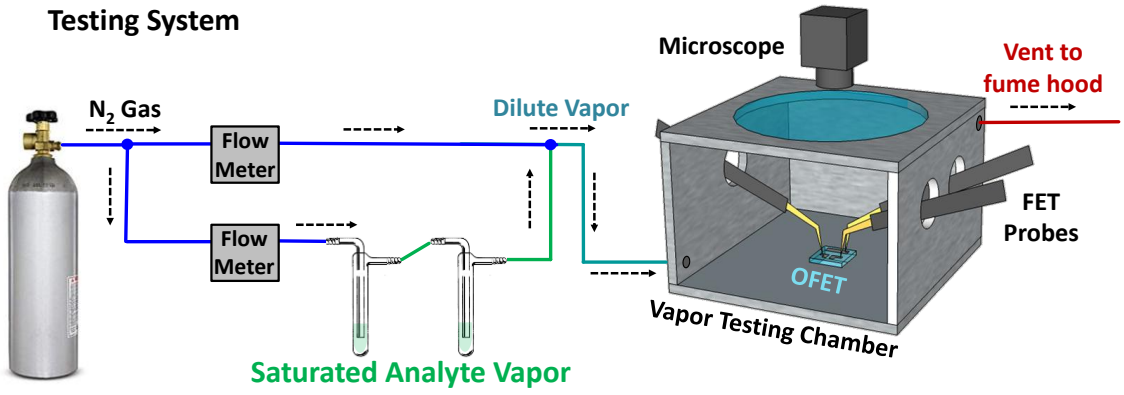

Figure 3. Schematic diagram showing the system used to generate a stream of nitrogen with controllable analyte concentration, connected to an FET testing chamber with a vent to a fume hood. Reproduced with permission from [9].

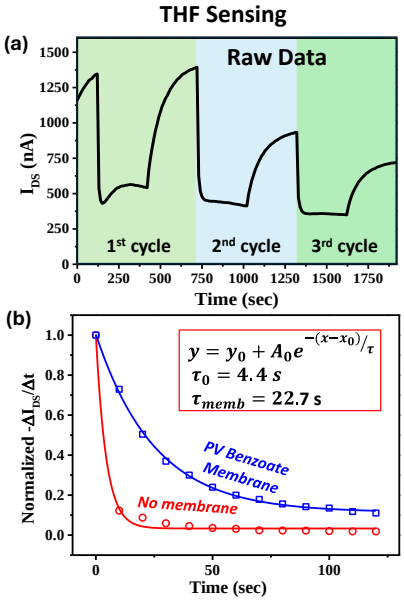

Figure 4. Sensing data. (a) Raw current versus time data for sensors repeatedly exposed to analyte (THF) vapor, followed by pure N_2 gas (3 repetitions). (b) Representative data for sensors with and without PVBenzoate membranes upon exposure to THF vapor after normalization and fitting with exponential decay curves.

dissimilarity, respectively.

Toluene and THF Sensing: Toluene, an aromatic VOC, interacted with PVBenzoate and PVCinnamate membranes via π-π interactions, resulting in distinct, delayed electrical responses. THF, which is a solvent for both PBTTT and the membrane polymers, showed relatively low selectivity enhancement with membranes, revealing that selectivity is best achieved when the membrane and sensing layers have dissimilar solubilities.

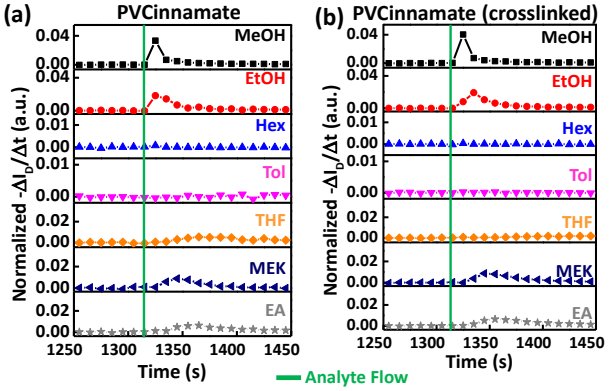

Figure 5. Representative sensing data comparing normalized ΔI/Δt vs t for sensors with (a) a PVCinnamate membrane and (b) a crosslinked PVCinnamate membrane upon exposure to seven different analytes. Reproduced with permission from [9].

Kinetic Analysis of Sensor Responses: Quantitative analysis of I_{DS} decay constants (τ_{decay}) confirmed that membranes slowed analyte diffusion into the sensing layer. For example, τ_decay for ethanol increased from 6.4 s in sensors without membranes to 16.0 s in PVBenzoate-coated sensors, demonstrating controlled transport kinetics. It should be noted that the film thickness has a minor effect on response time compared to the effect of chemical structure. The ability to modulate response times through membrane design introduces a new parameter for improving sensor selectivity.

Cross-Linked PVCinnamate for Enhanced Discrimination: Cross-linked PVCinnamate membranes exhibited the most pronounced selectivity effects. Compared to pristine PVCinnamate, cross-linked films increased ethanol response time (t_{peak}) from 10 s to 20 s and produced a more distinct response from methanol. These results suggest that cross-linking enhances selectivity by modulating diffusion pathways. A comparison of I_{DS} vs time for PVCinnamate and crosslinked

Table 1. Peak values (m_{peak}) of normalized rate of change in current ($\Delta I_{DS}/\Delta t$) for each combination of analyte and membrane. Percentages in brackets show the relative change m_{peak} compared to CP FETs with no membrane. Downward arrows (↓) indicate a relative decrease in current upon vapor exposure, upward arrows (↑) indicate a relative increase.

Analyte	Peak Rate of Change in Current (m_{peak}) Values (10^{-3}•s^{-1})					
	No Membrane	PVBenzoate	PVPalmitate	PVPivalate	PVCinnamate	PVCinnamate (cross-linked)
Methanol	49.7 ± 3.4	21.1 (42.5 %↓)	9.1 (18.3 %↓)	20.8 (41.9 %↓)	33.3 (67.0 %↓)	40.3 (81.1 %↓)
Ethanol	45.6 ± 3.5	22.5 (49.3 %↓)	11.0 (24.1 %↓)	13.1 (28.7 %↓)	18.3 (40.1 %↓)	19.2 (42.1 %↓)
Hexane	6.3 ± 0.7	-	- 1.4 (-22.2 %↑)	-	-	-
Toluene	10.6 ± 1.2	-	2.5 (23.6 %↓)	-	-	-
THF	32.4 ± 2.1	9.9 (30.6 %↓)	18.7 (57.7 %↓)	18.9 (58.3 %↓)	5.4 (16.7 %↓)	-
MEK	30.7 ± 3.7	15.5 (50.4 %↓)	26.8 (87.3 %↓)	21.9 (71.3 %↓)	8.9 (29.0 %↓)	8.7 (28.3 %↓)
Ethyl Acetate	29.6 ± 2.3	7.6 (25.7 %↓)	15.3 (51.7 %↓)	16.3 (55.1 %↓)	6.3 (21.9 %↓)	6.4 (21.6 %↓)

Table 2 Exponential decay time constant (τ_{decay}) of normalized $\Delta I_D / \Delta t$ (3rd cycle) for each combination of analyte and membrane.

Analyte	τ_{decay} (s)					
	No Membrane	PVBenzoate	PVPalmitate	PVPivalate	PVCinnamate	PVCinnamate (cross-linked)
Methanol	5.2 ± 0.4	14.4 ± 2.4	11.2 ± 0.6	11.1 ± 1.2	6.1 ± 0.4	5.5 ± 0.4
Ethanol	6.4 ± 0.2	16.0 ± 0.8	14.4 ± 1.5	9.0 ± 2.8	20.0 ± 0.4	15.9 ± 0.2
Hexane	10.6 ± 2.8	-	-	-	-	-
Toluene	13.7 ± 1.8	-	76.7 ± 5.6	-	-	-
THF	4.4 ± 0.4	25.4 ± 2.5	7.6 ± 0.4	13.1 ± 0.8	-	-
MEK	5.8 ± 0.3	10.9 ± 0.3	8.0 ± 0.5	11.1 ± 0.3	29.7 ± 3.9	42.0 ± 9.1
Ethyl Acetate	7.0 ± 0.4	16.9 ± 1.2	9.3 ± 1.3	11.9 ± 1.0	39.5 ± 0.6	50.9 ± 11.4

PVCinnamate membranes exposed to seven different analytes is shown in Figure 5.

Array-Based Sensing Approach: By analyzing the combined responses of multiple membrane-functionalized sensors, each VOC produced a unique pattern of electrical signals. This approach mimics biological olfaction, which relies on responses from hundreds or thousands of olfactory neurons, and enables reliable VOC identification with statistical confidence. When coupled with machine learning algorithms, such sensor arrays could provide a scalable route toward practical E-nose technologies.

Device Stability and Performance: Transfer and output curves confirmed that sensor performance remained stable after repeated analyte exposure. OFET mobility decreased slightly after extended testing but remained within functional limits. Membrane-coated devices exhibited lower degradation compared to uncoated sensors, suggesting that membranes also act as protective layers.

Summary of Sensor Characteristics: Summaries of quantitative characteristics (including peak current slope and time constants) for sensors with different membranes exposed to different analytes is shown in Table 1 and Table 2, respectively. Compared to devices with no membranes, a unique set of electrical responses is produced when the array of sensors with different membranes is exposed to each analyte. It should be emphasized that the sensors all relied on the same PBTTT detecting layer while the unique responses were elicited by the use of quickly and economically synthesized PVA membranes.

4. Conclusions

We have demonstrated that semi-permeable polymer membranes significantly enhance the selectivity of OFET vapor sensors. Membrane-functionalized sensors distinguished VOCs based on selective diffusion and unique electrical response profiles. This approach offers a scalable route to high-performance electronic noses without requiring complex synthesis of new conjugated polymers. Future work will explore a broader range of membrane structures and leverage computational modeling to optimize sensor selectivity. By integrating these advancements with artificial intelligence, practical and robust E-nose systems may soon be realized.

5. References

[1] F. Wen, T. He, H. Liu, H.Y. Chen, T. Zhang, C. Lee, Nano Energy 78 (2020) 105155.

[2] M. Meyyappan, Small 12 (2016) 2118–2129.

[3] F.J. Liao, UC Berkeley Electron. Theses Diss. (2009).

[4] A. Berna, Sensors 10 (2010) 3882–3910.

[5] A.D. Wilson, Metabolites 5 (2015) 140–163.

[6] H. Klauk, Chem. Soc. Rev. 39 (2010) 2643–2666.

[7] C. Zhang, P. Chen, W. Hu, Chem. Soc. Rev. 44 (2015) 2087–2107.

[8] J. del Mármol, M.A. Yedlin, V. Ruta, Nature 597 (2021) 126–131.

[9] J.Y. Kim, F. Haque, J.H. Lee, Y.J. Park, J.H. Seo, M. Mativenga, B. Walker, Appl. Mater. Today 37 (2024).